environmental sciences proceedings

MDPI

Proceeding Paper

ANALYSIS OF IONOSPHERIC MAPS DURING INTENSE GEOMAGNETIC STORMS (Dst≤-100nt) IN THE PERIOD 2011-2018.

Charbeth Lopez Urias[1]*, Karan Nayak[1], Guadalupe Esteban Vazquez Becerra[1], and Rebeca Lopez Montes[2]

[1] Faculty of Earth and Space Sciences, Autonomous University of Sinaloa, Mexico

[2] Department of Applied Geophysics, Center for Scientific Research and Higher Education of Ensenada, Mexico

* Correspondence: charbethlopez@uas.edu.mx

† Presented at the 6th International Electronic Conference on Atmospheric Sciences, 2023

Abstract: The layer of Earth's atmosphere known as the ionosphere presents a significant obstacle to global satellite navigation systems (GNSS) due to its ability to introduce errors. To address this challenge, various navigation systems have introduced new signals designed to minimize errors caused by the ionosphere. These signals not only aid in error reduction but also facilitate the examination of electron content behavior. This research focuses on the analysis of vTEC plots obtained from RINEX data collected at the INEG station in Aguascalientes, Mexico, from 2011 to 2018, with a particular emphasis on highly intense geomagnetic storms characterized by values below -100 nT. The analysis of these plots employs the Probability Density Function (PDF), which allows for the representation of data distribution on graphs. This distribution is then examined in conjunction with the station's Total Electron Content (TEC) values and the Dst index during the corresponding geomagnetic storm events. The findings establish the correlation between each of these parameters during such events.

Keywords: GNSS; Ionosphere; TEC; PDF

Citation: To be added by editorial staff during production.

Academic Editor: Firstname Lastname

Published: date

1. Introduction

The ionosphere's influence on Global Navigation Satellite Systems (GNSS) signals has long been recognized as a primary source of error in satellite-based positioning. However, its significance extends far beyond mere technical challenges, encompassing a pivotal role in global communications and a susceptibility to various factors, most notably, solar events [1]. Within the framework of GNSS, the dual-frequency capabilities of systems like GPS play a crucial role in characterizing ionospheric behavior. This capability allows the assessment of ionospheric effects and facilitates the determination of Total Electron Content (TEC), providing insights into electron density variations along the satellite-receiver path. Furthermore, the Sun, as a celestial powerhouse, exerts a profound influence on the ionosphere [1,2,3]. Solar phenomena such as coronal mass ejections, solar flares, and solar energetic particle events can instigate disruptive consequences, affecting telecommunications, radiocommunications, and satellite-based systems [4,5]. These objectives are designed to investigate ionospheric behavior during intense geomagnetic storms and to explore its interplay with solar and seasonal cycles. Drawing from historical context, we delve into the evolution of ionospheric research, its ionization processes, and the pivotal role that GNSS systems have played in advancing our comprehension of this enigmatic layer of Earth's atmosphere [1,6]. Furthermore, a hypothesis is formulated, suggesting that geomagnetic storms can induce significant ionospheric disturbances, and a statistical tool, the Probability Density Function (PDF), is proposed for event classification and analysis. By addressing these key aspects, this manuscript contributes to a deeper understanding of the ionosphere's multifaceted role and its implications for both navigation and global communication systems). With a focus on 22 intense geomagnetic storms occurring between 2011 and 2018, characterized by Dst index values of less than -100nT, this research aims to unravel the ionospheric behavior during these disruptive events. By investigating the interplay between geomagnetic storms, solar cycles, and seasonal variations, this manuscript seeks to advance our understanding of the ionosphere's multifaceted role, ultimately benefiting global navigation and communication systems.

2. Data Used and Methodology

In this study, data for the Dst index were acquired from the website of the Center for Data Analysis for Geomagnetism and Space Magnetism at the University of Kyoto. A Python code was developed to plot the data. The criteria for obtaining Dst index data focused on geomagnetic storms with Dst index values less than -100nT. After identifying the events, RINEX data for the selected station were downloaded, and the Total Electron Content (TEC) was calculated using GPSTEC software version 2.9.5. These TEC data were used to create vTEC plots. Subsequently, Probability Density Functions (PDFs) were applied to the ionospheric plots using MATLAB R2017b. The analysis involved categorizing ionospheric storms as positive or negative, examining maximum TEC values, minimum Dst index values, solar and seasonal cycles, and local time.

For TEC calculation, the dual-frequency nature of the GPS system was utilized to assess ionospheric effects. The Total Electron Content (TEC) can be calculated using phase measurements, where TEC = 9.52(R2 - R1), or pseudorange measurements, where TEC = 9.52(R2 - R1) [7]. The phase-based TEC calculation provides precise temporal variations, while the pseudorange method offers absolute values. The GPS observations were adjusted for satellite and receiver delays, multipath effects, and receiver noise [8]. Additionally, the PDF was used to analyze the probability distribution of variable values. The PDF identifies regions of higher and lower probabilities for a continuous random variable [9,10]. The PDF for a distribution can be obtained by differentiating the cumulative distribution function (CDF) [10]. The PDFs for transformed variables were computed using the Jacobian. Moments and statistics were also considered to derive asymptotic PDFs.

3. Results

3.1. Event 1 (August 6, 2011)

On August 6, 2011, a geomagnetic storm with a Dst index of -115 nT occurred, considered intense. Negative ionospheric disturbances were observed during this storm, with the day before recording a vTEC value of 35.34 TECU, while during and after the storm, values of 16.91 and 18.42 TECU were reached, respectively. The vTEC and Dst index graph for this event is shown in Figure 1. The Probability Density Function (PDF) results for this event, displayed in Figure 1, demonstrate the range of vTEC values before, during, and after the event.

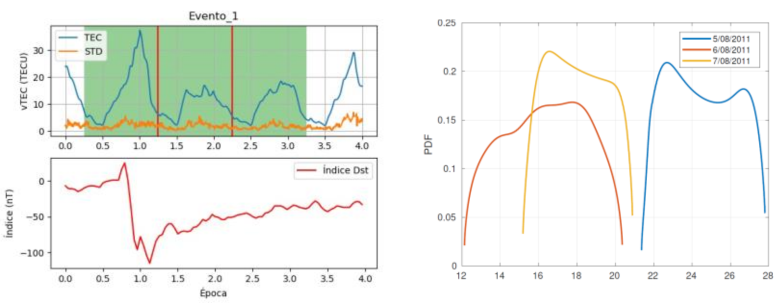

Figure 1. vTEC response to Event 1 - PDF Analysis.

3.2. Event 2 (September 26, 2011)

The September 26, 2011 storms caused significant ionospheric alterations, with vTEC values reaching 77.32 TECU during the storm. Before the storm, TEC values were 40.01 TECU, and they quickly recovered to 39.29 TECU after the storm, indicating a positive ionospheric storm. Although intense, this geomagnetic storm had a Dst index of -118 nT, suggesting it was not as perturbing as other events from the same solar cycle. Figure 2 illustrates the variations in vTEC and the geomagnetic index for this event. The PDF results in Figure 2 show uniform alterations in vTEC throughout the study region during the event.

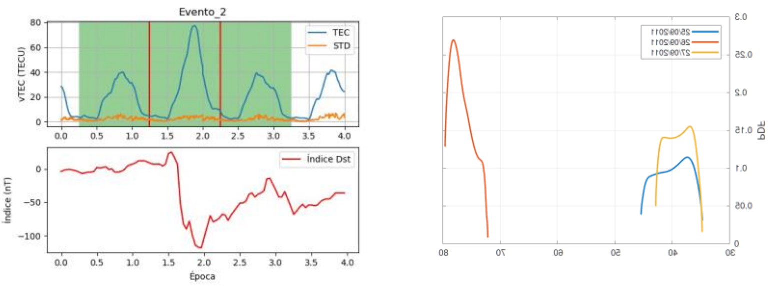

Figure 2. vTEC response to Event 2 - PDF Analysis.

3.3. Event 3 (October 25, 2011)

On October 25, 2011, the strongest geomagnetic storm of 2011 occurred, with a Dst index reaching -134 nT and peaking at 6:00 UT. This storm led to positive ionospheric disturbances, as evident in Figure 3, along with an increase in standard deviation. Interestingly, the largest data dispersion is not observed at the peak of the storm but rather during other times. Figure 3 shows the PDF results for this event, highlighting the vTEC increase in the study region, with a small area preserving its previous values due to their uniformity the day before the storm.

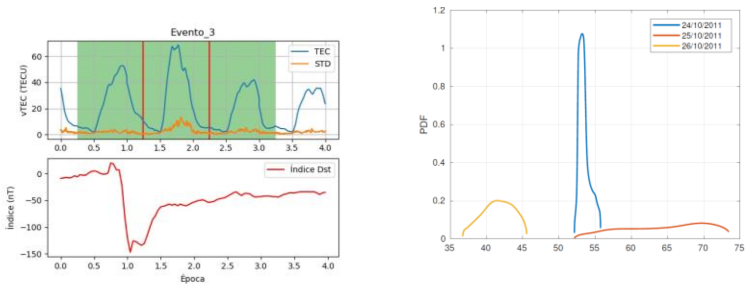

Figure 3. vTEC response to Event 3 - PDF Analysis.

3.4. Event 4 (March 9, 2012)

The event on March 9, 2012, had an intensity of -145 nT, peaking at 9:00 UT. Despite ranking as the fifth most intense storm of Solar Cycle 24, it resulted in negative ionospheric disturbances, as shown in Figure 4. The PDF results in Figure 4 reveal changes in vTEC range during the event. Although the ionosphere experienced higher variations in the region after the event, recovery was rapid, as it only negatively impacted the ionosphere for one day.

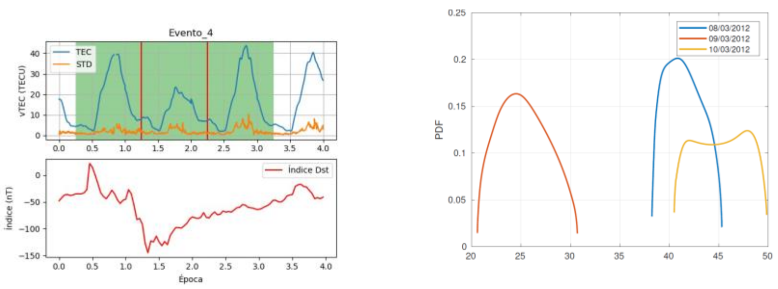

Figure 4. vTEC response to Event 4 - PDF Analysis

The subsequent occurrences are detailed in the table beneath, along with their respective repercussions on the ionosphere.

Table 1. Table of Events and their Effects on the Ionosphere

Event	Date	Day Cycle	Dst Index	vTEC Impact
5	April 24, 2012	Night	-120nT	Negative
6	July 15, 2012	Day	-140nT	Negative
7	October 1, 2012	Night	-120nT	Negative
8	October 9, 2012	Night	-110nT	Positive, Negative
9	November 14, 2012	Night	-110nT	Positive
10	March 17, 2013	Day	-150nT	Positive
11	June 1, 2013	Night	-124nT	Negative
12	June 29, 2013	Night	-102nT	Negative
13	February 19, 2014	Night	-119nT	Positive
14	March 17, 2015	Day	-222nT	Positive
15	June 23, 2015	Night	-204nT	Negative
16	October 7, 2015	Day	-124nT	Positive
17	December 20, 2015	Day	-155nT	Positive
18	January 1, 2016	Night	-110nT	Positive, Negative
19	October 13, 2016	Day	-104nT	Positive
20	May 28, 2017	Night	-125nT	Positive, Negative
21	September 8, 2017	Night	-124nT	Negative
22	August 26, 2018	Night	-174nT	Negative

Across various geomagnetic events, notable fluctuations in the Total Electron Content (TEC) and the Dst index were observed. Event 5, on April 24, 2012, had a Dst Index of -120 nT and negatively impacted the ionosphere, with TEC changing from 59.29 TECU before the storm to 50.32 TECU during and 56.03 TECU after. Event 6, on July 15, 2012, had a unique ionospheric behavior with slow recovery, and Event 7, on October 1, 2012, negatively affected the ionosphere during the day, reaching 33.38 TECU. Event 8, on October 9, 2012, had varying impacts on the ionosphere over three days. Event 9, on November 14, 2012, was positively influenced, with TEC increasing from 37.70 TECU before the storm to 54.94 TECU during. Finally, Event 10, on March 17, 2013, had a positive impact, with TEC rising from 43.80 TECU before the storm to 80.93 TECU during. Event 11, on June 1, 2013, had a unique pattern with a negative impact, causing slow recovery in the ionosphere. These events highlight the varying effects of geomagnetic storms on the ionosphere's Total Electron Content. Event 12 on June 29, 2013, showcased a significant negative impact on TEC, reaching its lowest point (-102 nT) at 7:00hrs UTC, with a nighttime peak. This storm hindered ionospheric recovery, leading to relatively low TEC values during the day, with a minor nighttime increase noted at the end of June 28, 2013. Event 13 (February 19, 2014) coincided with heightened solar activity but displayed a positive TEC response, peaking at 65.00 TECU during the storm and reverting to 50.08 TECU afterward.

Event 14 (March 17, 2015), the most intense of Solar Cycle 24 with a Dst of -222 nT, caused notable TEC variations. It decreased during the day and rose in the evening, impacting the ionosphere even post-storm. Event 15 (June 23, 2015), the second most intense of the cycle, brought about a severe negative ionospheric effect, with TEC values declining from 55.59 TECU to 34.05 TECU, showing limited recovery. Event 16 (October 7, 2015) led to a positive ionospheric response, but TEC dispersion varied across the day. Event 17 (December 20, 2015) exhibited a positive ionospheric effect, with TEC rising from 30.45 TECU to 49.16 TECU during the storm. Event 18 (January 1, 2016) displayed mixed results, making the ionospheric impact unclear. Event 19 (October 13, 2016) had a positive ionospheric influence, with TEC rising from 23.12 TECU to 55.99 TECU. Event 20 (May 28, 2017) showed nighttime TEC increases during the storm but had an overall negative ionospheric impact. Event 21 (September 8, 2017) led to reduced TEC values throughout the storm. Finally, Event 22 (August 26, 2018), the last of Solar Cycle 24, had a predominantly negative ionospheric impact. These events highlight the complex relationship between geomagnetic storms and ionospheric behavior, with some storms causing positive responses, while others induce negative and lasting effects on TEC.

4. Conclusions

Solar activity, indicated by sunspots, can increase the likelihood of geomagnetic storms, but the intensity of these storms does not necessarily correlate with sunspot quantity, as demonstrated by Event 22 in August 2018, occurring during a solar cycle minimum yet being notably intense. These storms can affect the ionosphere, leading to positive or negative disturbances. Some events, such as 4 (March 9, 2012), 5 (April 24, 2012), and 20 (May 28, 2017), show nighttime disturbances indicating a potential positive impact, while daytime disruptions, as seen in events like 15 (June 23, 2015), suggest a negative effect. The timing of storm peaks plays a crucial role, with daytime peaks often resulting in positive ionospheric storms. Seasonality also influences ionospheric responses, with winter storms like 10 (March 17, 2013) predominantly causing positive impacts, while spring events like 5 (April 24, 2012) and 11 (June 1, 2013) show negative daytime effects. Overall, understanding the complex relationship between solar activity, geomagnetic storms, and ionospheric disturbances is vital for space weather research and risk assessment.

Author Contributions: Conceptualization, C.L.U. and K.N.; methodology, C.L.U.; software, K.N.; validation, K.N., C.L.U., and G.E.V.B.; formal analysis, R.L.M.; investigation, C.L.U.; resources, K.N.; data curation, C.L.U.; writing—original draft preparation, C.L.U.; writing—review and editing, K.N.; visualization, G.E.V.B.; supervision, R.L.M.; project administration, G.E.V.B.; funding acquisition, C.L.U. All authors have read and agreed to the published version of the manuscript.

Funding: This work was carried out with the support (CVU: 859540) of the National Council of Science and Technology (CONACyT) in Mexico.

Data Availability Statement: The data can be made available on request.

Acknowledgments: The authors would like to thank the Center for Data Analysis for Geomagnetism and Space Magnetism at the University of Kyoto for making the data readily available. The authors further extend their heartfelt thanks to CONACYT (National Council for Science and Technology) for their financial support that made this research possible

Conflicts of Interest: The authors declare no conflict of interest.

References

1. López-Urias, C.; Vazquez-Becerra, G.E.; Nayak, K.; López-Montes, R. Analysis of Ionospheric Disturbances during X-Class Solar Flares (2021–2022) Using GNSS Data and Wavelet Analysis. Remote Sens. 2023, 15, 4626. https://doi.org/10.3390/rs15184626
2. Nishimoto, S.; Watanabe, K.; Kawai, T.; Imada, S.; Kawate, T. Validation of computed extreme ultraviolet emission spectra during solar flares. Earth Planets Space 2021, 73, 79.
3. Yasyukevich, Y.; Astafyeva, E.; Padokhin, A.; Ivanova, V.; Syrovatskii, S.; Podlesnyi, A. The 6 September 2017 X-class solar flares and their impacts on the ionosphere, GNSS, and HF radio wave propagation. Space Weather 2018, 16, 1013–1027.

4. Marov, M.Y., Kuznetsov, V.D. (2015). Solar Flares and Impact on Earth. In: Pelton, J., Allahdadi, F. (eds) Handbook of Cosmic Hazards and Planetary Defense. Springer, Cham. https://doi.org/10.1007/978-3-319-03952-7_1
5. Singh, A.K.; Bhargawa, A.; Siingh, D.; Singh, R.P. Physics of Space Weather Phenomena: A Review. Geosciences 2021, 11, 286. https://doi.org/10.3390/geosciences11070286
6. Liu, J.-Y.; Lin, C.-H.; Rajesh, P.K.; Lin, C.-Y.; Chang, F.-Y.; Lee, I.-T.; Fang, T.-W.; Fuller-Rowell, D.; Chen, S.-P. Advances in Ionospheric Space Weather by Using FORMOSAT-7/COSMIC-2 GNSS Radio Occultations. Atmosphere 2022, 13, 858. https://doi.org/10.3390/atmos13060858
7. Araujo-Pradere, E. A. "GPS-derived total electron content response for the Bastille Day magnetic storm of 2000 at a low mid-latitude station." Geofísica internacional 44.2 (2005): 211-218.
8. Wanninger, L., Sumaya, H. & Beer, S. Group delay variations of GPS transmitting and receiving antennas. J Geod 91, 1099–1116 (2017). https://doi.org/10.1007/s00190-017-1012-3
9. Seifedine Kadry and Khaled Smaily, 2007. Using the Transformation Method to Evaluate The Probability Density Function of z = xα yβ. The International Journal of Applied Economics and Finance, 1: 105-112.
10. Taylor, C. Robert. "A flexible method for empirically estimating probability functions." Western Journal of Agricultural Economics (1984): 66-76.